

High-efficiency Optical Phase Conjugation in a single Ultra-low-loss Silicon Waveguide for Nonlinearity Compensation

Shihan Hong⁽¹⁾, Mingming Tan⁽²⁾, Andrew D. Ellis⁽²⁾, Abdallah Ali⁽²⁾, Long Zhang⁽¹⁾, Mingfei Ding⁽¹⁾, Shujun Liu⁽¹⁾, Baobao Chen⁽¹⁾, Zhihuan Ding⁽¹⁾, Gangmin Li⁽¹⁾, Yiwei Xie^{*(1,3)}, Daoxin Dai^(1,3)

- (1) Centre for Optical and Electromagnetic Research, Zhejiang University, Hangzhou, Zhejiang, 310058, China, xieyw@zju.edu.cn.
 (2) Aston Institute of Photonic Technologies, Aston University, Birmingham B4 7ET, U.K.
 (3) Ningbo Research Institute, Zhejiang University, Ningbo 315100, China.

Abstract We demonstrate the optical phase conjugation technique using a silicon spiral waveguide fabricated by standard multi-project-wafer processes with ultralow loss of 0.285 dB/cm, high conversion efficiency of -8 dB and evaluate the performance with a 20 Gb/s QPSK signal.

Introduction

Digital [1] and all-optical [2] approaches have been reported to tackle the nonlinearity caused by the require higher launched power for achieving a high optical signal-to-noise ratio (OSNR) in current optical communication systems. Among them, optical phase conjugation (OPC) is widely known as a promising solution in both optical fibre [3] and free-space communication link [4] thanks to the inherent broader bandwidths characteristic of optical methods and easy implementation in nonlinear media. So far, successful demonstrations have been reported using highly nonlinear fibres (HNLFs) [2-4] and periodically poled lithium niobite (PPLN) waveguides [5]. However, these approaches either have large footprints or need high operation temperature.. Meanwhile, silicon photonic devices have been extensively investigated for OPC [6-9] owing to their high integration, CMOS compatibility and unrivalled nonlinearities. However, the strong two photon absorption (TPA) and TPA-induced free carrier absorption (FCA) of silicon pose a fundamental limitation to nonlinear signal processing and the conversion efficiency (CE) is below 20 dB [6, 7]. Though the nonlinear loss due to the FCA can be reduced by sweeping the free carriers by using a p-i-n junction [8, 9], it requires complex fabrication processes which introduce high cost and external power supply. One should note that in addition to the nonlinear loss, the linear propagation loss will also limit the wavelength conversion. However, there is still several dB/cm of propagation loss for the standard singlemode waveguide under current process conditions.

In this paper, we propose an ultra-low-loss spiral waveguide with standard multi-project-wafer (MPW) processes on the silicon-on-insulator (SOI). To reduce the scattering loss in the sidewall, the width of the waveguide is optimized to 2 μm so that the propagation loss is decreased

to 0.28 dB/cm. Moreover, Archimedean spiral and tapered Euler-curve S-bend techniques are applied to ensure the negligible mode mismatch as well as high-order mode excitation. As a result, a longer effective length L_{eff} can be achieved by the low-loss propagation which leads to a CE as high as -8 dB and preponderated over -15 dB in the wavelength detuning of ± 10 nm in the 20-cm long spiral. Furthermore, the OSNR-dependent Q-factor penalty of the conjugates is demonstrated with respect to the back-to back performance with 20 Gb/s quadrature phase-shift keying (QPSK) signal, and the conjugates shows an average penalty of < 1 dB within OSNR ranging from 10 to 15 dB.

Principle

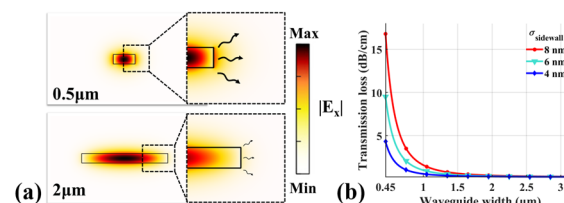


Fig. 1: The calculated field profiles for a singlemode waveguide (0.5 μm) and multimode waveguide (2 μm) with $H_{\text{wg}} = 0.22\mu\text{m}$. The dashed boxes show the enlarged field profiles at waveguide edges.

As is known to all, the scattering loss caused by the unsmooth surfaces, especially the sidewalls, dominates the waveguide's linear propagation loss. As shown in Fig. 1(a), compared with the single mode waveguide ($W_{\text{sm}} = 0.5 \mu\text{m}$), the evanescent field in the sidewall of is much weaker than the broadened multimode waveguide ($W_{\text{mm}} = 2 \mu\text{m}$), resulting in a lower scattering loss. Under existing fabrication level, the sidewall roughness σ_{sidewall} customarily ranges from 3 nm to 10 nm. Here, a three-dimensional volume current method [10] was introduced to quantify the scattering loss at the waveguide interfaces, which is the major loss

source, as shown in Fig. 1(b). In this case, we assume mean square deviation of the sidewall roughness $\sigma_{\text{sidewall}} = 8 \text{ nm}$, 6 nm , 4 nm . It can be seen that σ_{sidewall} plays a significant part when the waveguide core width W_{co} of the waveguide is narrow. However, for $W_{\text{co}} > 2 \mu\text{m}$, the scattering loss becomes insensitive to the core width and σ_{sidewall} . Therefore, the multimode waveguide width in this work is chosen as $W_{\text{co}} = 2 \mu\text{m}$.

Characterization of propagation loss and conversion efficiency

The microscope image of the fabricated 20-cm silicon waveguide spiral is shown in Fig. 2(a). The spiral waveguides are assisted with the Archimedean spiral and tapered Euler-curve S-bend to ensure the smooth gradient between different radius waveguide, and therefore high-order mode excitation can be avoided. The propagation loss is characterized by measuring different lengths of the spiral and the results are shown in Fig. 2(b). It can be seen that the losses are wavelength-independent in the C-band and the fitting result shows that the measured waveguide loss is $\sim 0.285 \text{ dB/cm}$ at 1550 nm , which is almost ~ 20 time smaller than that of the singlemode waveguide in the same chip ($2\text{-}3 \text{ dB/cm}$).

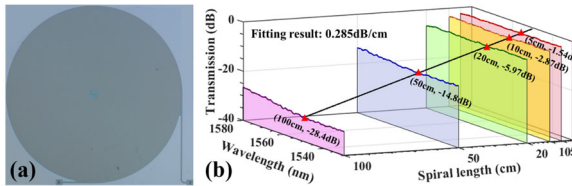


Fig. 2: (a) Microscope image of the fabricated waveguide spiral. (b) Measured transmissions of the waveguide spirals with different lengths $L = 5, 10, 20, 50,$ and 100 cm and the fitting loss at 1550 nm .

The following wavelength conversion experiment is carried on by the $2\text{-}\mu\text{m}$ -width, 20-cm -long spiral waveguide with an input pump power of 25 dBm at 1550.1 nm , signal power of 14 dBm at 1549.3 nm and the output spectra is shown in Fig. 3(a). The four-wave mixing (FWM) process is observed in the output spectra and the CE of the idler converted at 1550.9 nm is as high as -8 dB with OSNR at 33 dB . To the best of our knowledge, it's the highest CE of the continuous-wave pumped FWM in the passive SOI at C-band. The output signal power to the waveguide is limited by the low chip-fiber grating coupler coupling efficiency. Fortunately, this can be improved by using edge couplers. Additionally, the wavelength-dependence of the CE is described in Fig. 3(b) when the pump is fixed at 1550.1 nm . It can be seen that the CE is above -15 dB in the wavelength detuning of $\pm 10 \text{ nm}$.

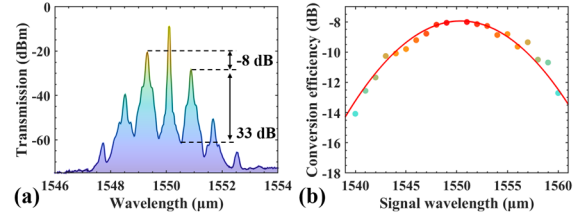


Fig. 3: (a) The output spectra of the spiral waveguide with pump power of 25 dBm at 1550.1 nm , signal power of 14 dBm at 1549.3 nm . (b) The conversion efficiency spectra at different signal wavelength with fixed pump wavelength.

OPC performance

The experiment setup of the OPC stage based on low-loss silicon waveguide for evaluating the performance of the converted idler is shown in Fig. 4. In the transmitter, the signal is launched by a continuous-wave (CW) laser at 1549.3 nm , and then modulated by an IQ modulated (Fujitsu FTM7962) driven by two 10 Gb/s $2^{15}\text{-}1$ pseudo-random binary sequences (PRBSs) generated from a BPG to achieve 20 Gb/s QPSK signal. EDFA1 is used to compensate the loss of the modulator. The amplified signal is then combined with the pump generated by a distributed feedback (DFB) lasers at 1550.1 nm through a WDM and coupled into the chip through the grating couplers. The pump is also amplified by EDFA2 to receive enough nonlinear effect in the silicon waveguides. The polarizations of the pump and signal at the input of the chip are controlled by a PC for TE mode in order to maximize the FWM conversion efficiency. The broadband noise source ASE is coupled with a $1:9$ coupler to control the OSNR of the link at the output of the chip. The idler wavelengths are selected by the OBPF and received by the polarization and phase-diverse coherent detection after the pre-amplifier. At the receiver, the signals are undergoing analog-to-digital conversions by a 50-Gsamples/s sampling rate digital serial analyzer (Tektronix, DSA 72004C) followed by off-line digital signal processing (DSP). More than 500 k symbols were averaged and processed and the performance was characterized by measuring the Q factor of the resulting constellation.

As shown in Figure 5, the Q^2 of the idler against OSNR for the conjugates with respect to that of the back-to-back system. Here launched powers of the pump and signal are consistent with that in Fig. 3. It can be seen that the Q^2 penalty of conjugates with respect to the back-to-back performance is below 1 dB within the OSNR range. At the low OSNR ($\sim 10 \text{ dB}$), the conjugates have a very negligible penalty of below 0.1 dB , this is mainly because the added ASE noise

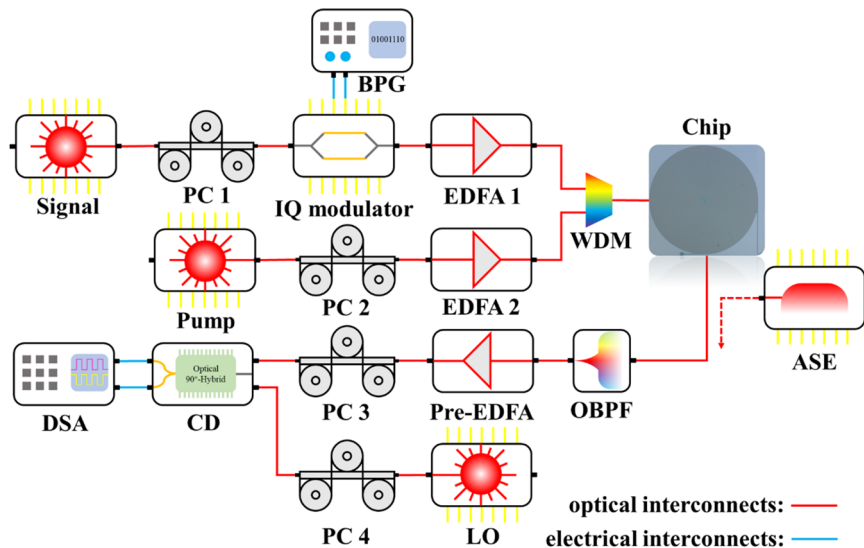


Fig. 4: (a) Experimental setup for benchmarking the performance of the wavelength converted idler against the original (back-to-back) signal. PC, polarization controller. BPG: Bit-pattern generator. IQ modulator: in phase/quadrature modulator. EDFA: erbium-doped fiber amplifier. WDM: wavelength division multiplexer. ASE: amplified-spontaneous-emission source. OBPf: optical bandpass filter. LO: local oscillator. CD: Coherent detector. DSA: Digital Serial analyzer. The red lines represent optical interconnects, while the blue lines represent electrical interconnects.

contributes to the system performance. At higher OSNRs (20dB) the average penalty increased to a mean of ~ 1 dB, due to the unwanted four wave mixing products. The results show that the implementation of this OPC subsystem within a mid-span arrangement where the OSNR would be necessarily low. The corresponding constellation diagrams at OSNR ~ 13.5 dB are demonstrated in the inset.

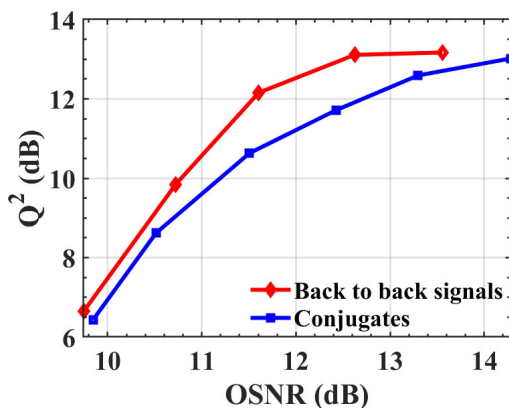


Fig. 5: Q^2 versus receiver OSNR for back to back signal and respective conjugates. Inset shows the constellation diagrams of the at OSNR ~ 13.5 dB.

Conclusions

As a conclusion, we have proposed an ultra-low-loss and high CE SOI spiral waveguide for OPC application by standard MPW foundry. By analysing the scattering loss caused by the sidewalls, it is demonstrated that the broadened core width of the waveguide can reduce the propagation loss effectively. Additionally, to avoid

high-order mode excitation as well as compactness, the assisted Archimedean spiral and tapered Euler-curve S-bend are introduced in the spiral design. The measured spectra result of different length spirals reveals a propagation loss of 0.28 dB/cm in the C-band. For the 20-cm long spiral, the measured CE is as high as -8 dB and preponderated over -15 dB in the wavelength detuning of ± 10 nm. Finally, the performance of the wavelength converted idler against the back-to-back (BTB) signal with 20 Gb/s QPSK signal was demonstrated and the feasibility of low-loss silicon waveguide for the OPC application was verified.

Acknowledgements

We are grateful for financial supports from National Major Research and Development Program (No. 2018YFB2200200); National Science Fund for Distinguished Young Scholars (61725503); Zhejiang Provincial Natural Science Foundation (LZ18F050001, LGF21F050003); National Natural Science Foundation of China (NSFC) (91950205, 6191101294, 11861121002, 61905209, 62175214, 62111530147); Royal Society International Exchange Grant (IEC\NSFC\201406) and the EPSRC, grants EP/S003436/1 (PHOS) and EP/V000969/1 (ARGON).

References

- [1]. E. Ip, "Nonlinear Compensation Using Backpropagation for Polarization-Multiplexed Transmission," *Journal of Lightwave Technology*, 2010, 28(6), 939-951. <http://dx.doi.org/10.1109/jlt.2010.2040135>

- [2]. P. Minzioni, "Nonlinearity Compensation in a Fiber-Optic Link by Optical Phase Conjugation," *Fiber and Integrated Optics*, 2009, 28(3), 179-209. <http://dx.doi.org/10.1080/01468030802364117>
- [3]. M. F. Stephens, M. Tan, I. D. Phillips, S. Sygletos, P. Harper and N. J. Doran, "1.14 Tb/s DP-QPSK WDM polarization-diverse optical phase conjugation," *Opt Express*, 2014, 22(10), 11840-11848. <http://dx.doi.org/10.1364/OE.22.011840>
- [4]. J. Chen, Z. Yu, T. Wang, Z. Liu and S. Gao, "Demonstration of an optical phase conjugation based dual-hop PDM-QPSK free-space optical communication link," *Electronics Letters*, 2022, 58(6), 252-254. <http://dx.doi.org/10.1049/el2.12421>
- [5]. M. H. Chou, K. R. Parameswaran, M. M. Fejer and I. Brener, "Multiple-channel wavelength conversion by use of engineered quasi-phase-matching structures in LiNbO₃ waveguides," *Opt Lett*, 1999, 24(16), 1157-1159. <http://dx.doi.org/10.1364/ol.24.001157>
- [6]. S. Ayotte, S. Xu, H. Rong, O. Cohen and M. J. Paniccia, "Dispersion compensation by optical phase conjugation in silicon waveguide," *Electronics Letters*, 2007, 43(19). <http://dx.doi.org/10.1049/el:20071506>
- [7]. D. Vukovic, J. Schroder, F. Da Ros, L. B. Du, C. J. Chae, D. Y. Choi, M. D. Pelusi and C. Peucheret, "Multichannel nonlinear distortion compensation using optical phase conjugation in a silicon nanowire," *Opt Express*, 2015, 23(3), 3640-3646. <http://dx.doi.org/10.1364/OE.23.003640>
- [8]. F. Da Ros, A. Gajda, E. P. da Silva, A. Peczek, A. Mai, K. Petermann, L. Zimmermann, L. K. Oxenlowe and M. Galili, "Optical Phase Conjugation in a Silicon Waveguide With Lateral p-i-n Diode for Nonlinearity Compensation," *Journal of Lightwave Technology*, 2019, 37(2), 323-329. <http://dx.doi.org/10.1109/jlt.2018.2873684>
- [9]. F. Da Ros, A. Gajda, E. Liebig, E. P. da Silva, A. Peczek, P. D. Girouard, A. Mai, K. Petermann, L. Zimmermann, M. Galili and L. K. Oxenlowe, "Dual-polarization wavelength conversion of 16-QAM signals in a single silicon waveguide with a lateral p-i-n diode [Invited]," *Photonics Research*, 2018, 6(5). <http://dx.doi.org/10.1364/prj.6.000b23>
- [10]. J. F. Bauters, M. J. Heck, D. John, D. Dai, M. C. Tien, J. S. Barton, A. Leinse, R. G. Heideman, D. J. Blumenthal and J. E. Bowers, "Ultra-low-loss high-aspect-ratio Si₃N₄ waveguides," *Opt Express*, 2011, 19(4), 3163-3174. <http://dx.doi.org/10.1364/OE.19.003163>